Modulation of Microtubule Interprotofilament Interactions by Modified Taxanes

Ruth Matesanz,[†] Javier Rodríguez-Salarichs,[†‡] Benet Pera,[†] Angeles Canales,[†§] José Manuel Andreu,[†] Jesús Jiménez-Barbero,[†] Wim Bras,[¶] Aurora Nogales,[‖] Wei-Shuo Fang,[**] and José Fernando Díaz[†]

[†]Chemical and Physical Biology, Centro de Investigaciones Biológicas, Consejo Superior de Investigaciones Científicas CIB-CSIC, Madrid, Spain; [‡]Centro de Estudios Avanzados de Cuba, Carretera San Antonio, Valle Grande, La Lisa, Ciudad Habana, Cuba; [§]Departamento de Química Orgánica I, Facultad Ciencias Químicas, Universidad Complutense de Madrid, Madrid, Spain; [¶]Nederlandse Organisatie voor Wetenschappelijk Onderzoek (NWO), DUBBLE CRG/ESRF, Grenoble, France; [‖]Instituto de Estructura de la Materia, Consejo Superior de Investigaciones Científicas IEM-CSIC, Madrid, Spain; and [**]State Key Laboratory of Bioactive Substances and Functions of Natural Medicines, Institute of Materia Medica, Chinese Academy of Medical Sciences & Peking Union Medical College, Beijing, China

Supplementary Methods

X-ray scattering measurements.

For the BM26B station, the camera was set to cover the scattering vector range, defined as reciprocal Bragg spacing i.e. $s = 2 \sin \theta/\lambda$, from 0.01 to 0.40 nm^{-1}. Calibration of the scattering vector was obtained by reference to the orders of diffraction of silver behenate (1). The temperature of the samples was set to 25ºC and the X-Ray scattering profiles were recorded for 10 minutes in 15-second frames with a multiwire gas-filled 2D detector. Data analysis was performed using the FIT2D software package provided by ESRF http://www.esrf.eu/computing/scientific/FIT2D/. Raw data were normalized for beam intensity decay and detector response before averaging and subtracting the buffer scattering pattern. Time frames in which the data significantly differed from the original pattern due to radiation damage were removed before averaging. For the data collected with the Bruker NANOSTAR system the following differences apply: the camera was set to cover ranges of the scattering vector from 0.013 to 0.22 nm^{-1}, and the X-Ray scattering profile was recorded for 2 hours in 30-minute frames with a Bruker Hi-Star multiwire area detector.

Docking

Docking of the ligands was performed using the AutoDock 4.0 program (2). Atomic coordinates for the ligands were obtained from the NMR data assisted by molecular mechanics calculations (see above). The α/β-tubulin dimer coordinates were obtained from the Protein Data Bank 1JFF code. Model tetramer coordinates were kindly provided by Prof. M. Botta (3).

Since the scoring function implemented in the Autodock program was not useful to select a docking pose compatible with the experimental STD NMR results, a new scoring function (SF) was implemented, based on the difference between the experimental and theoretical STD of each ligand's proton (4). An in-house script which employs custom-made programs written in Fortran90 (to be published elsewhere) allowed the performance of exhaustive file treatment in order to score the docked conformations using the CORCEMA-ST program (5), therefore allowing the prediction of the STD values for a given ligand-receptor complex. Protein residues located inside a sphere of 8 Å around the ligand were considered for the calculations.

Table S1.- Conformational parameters of the ligands bound in the models constructed

Pore site

	T-Taxol[a]	Cephalomannine	Chitax-1	Chitax-17	Chitax-4	Docetaxel	Flutax-2
R1	9.4	8±1	6.0±0,4	7±2	11±1	7.9±0,9	8±2
R2	10	10.1±0.7	9.3±0,5	9.6±0,6	10.5±0,7	10.7±0,7	9.6±0,7
Phi1	80	67±8	66±9	70±20	90±20	89±8	60±10
Phi2	-58	-90±10	-70±10	-80±20	-80±10	-40±10	-90±10

Luminal site

	T-Taxol[a]	Cephalomannine	Chitax-1	Chitax-17	Chitax-4	Docetaxel	Paclitaxel
R1	9.4	5,9±0.4	11.1±0,8	9.7±0.6	6.0±0.7	9.0±0.9	12.5±0,7
R2	10	9,2±04	9.9±0,8	10.5±0,5	9.3±0,3	9±1	10.6±0,5
Phi1	80	61±6	100±10	70±10	57±8	94±9	100±10
Phi2	-58	-60±10	-60±10	-90±10	-70±10	-50±10	-66±7

[a]As defined in (6) improper torsion angles O-C2-C39-N(Bz) and O-C2-C39-C(Ph) (Phi1, Phi2). R1 and R2 are the distances (in angstroms) from the center of the C-2 benzoyl phenyl ring and the center of the C-3´ phenyl ring corresponding to the appropriate Phi1 and Phi2.

References

1. Huang, T. C., H. Toraya, T. N. Blanton, and Y. Wu. 1993. X-ray-powder diffraction analysis of silver behenate, a possible low-angle diffraction standard. J. Appl. Crystallogr. 26:180-184.
2. Morris, G. M., D. S. Goodsell, R. S. Halliday, R. Huey, W. E. Hart, R. K. Belew, and A. J. Olson. 1998. Automated docking using a Lamarckian genetic algorithm and an empirical binding free energy function. J Comput Chem 19:1639-1662.
3. Magnani, M., G. Maccari, J. M. Andreu, J. F. Diaz, and M. Botta. 2009. Possible binding site for paclitaxel at microtubule pores. FEBS J 276:2701-2712.
4. Canales, A., J. R. Salarichs, C. Trigili, L. Nieto, C. Coderch, J. M. Andreu, I. Paterson, J. Jiménez-Barbero, and J. F. Díaz. 2011. Insights into the interaction of discodermolide and docetaxel with dimeric tubulin. Mapping the binding sites of microtubule-stabilizing agents using an integrated NMR and computational approach. ACS Chemical Biology 6:789-799.
5. Jayalakshmi, V., and N. R. Krishna. 2002. Complete relaxation and conformational exchange matrix (CORCEMA) analysis of intermolecular saturation transfer effects in reversibly forming ligand-receptor complexes. J Magn Reson 155:106-118.
6. Snyder, J. P., J. H. Nettles, B. Cornett, K. H. Downing, and E. Nogales. 2001. The binding conformation of Taxol in beta-tubulin: A model based on electron crystallographic density. Proc Natl Acad Sci U S A 98:5312-5316.

Supplementary Figure Legends

Figure S1.- TR-NOESY spectra (mixing time: 200 ms) of Flutax-2 in the presence of microtubules (D_2O, 310 K). Relevant negative crosspeaks are labeled.

Figure S2.- Panel A.- Positions of the terminal carbon of the substituents at C7 and C10 for cephalomannine, Chitax-1, and Flutax-2 bound at the pore site. (Yellow points, position of the terminal carbon of the R10 side chain of cephalomaninne, green points position of the terminal carbon of the R7 side chain of Chitax-1, blue points position of the AC-($HCCH_3$)-NH of R7 side chain of Flutax-2. Magenta H3 Helix of β-tubulin subunit at the right side of the pore, White S3 of β-tubulin subunit at the right side of the pore). Panel B.-Comparison of the average conformation of β-tubulin M-loop in the models of the ligands bound to the luminal site, ligand (blue) cephalomannine, yellow loop, M-loop conformation with cephalomannine bound, white loop, M-loop conformation with Chitax-17 bound, green loop, M-loop conformation with Chitax-1 bound, blue loop, M-loop conformation with Chitax-4 bound.

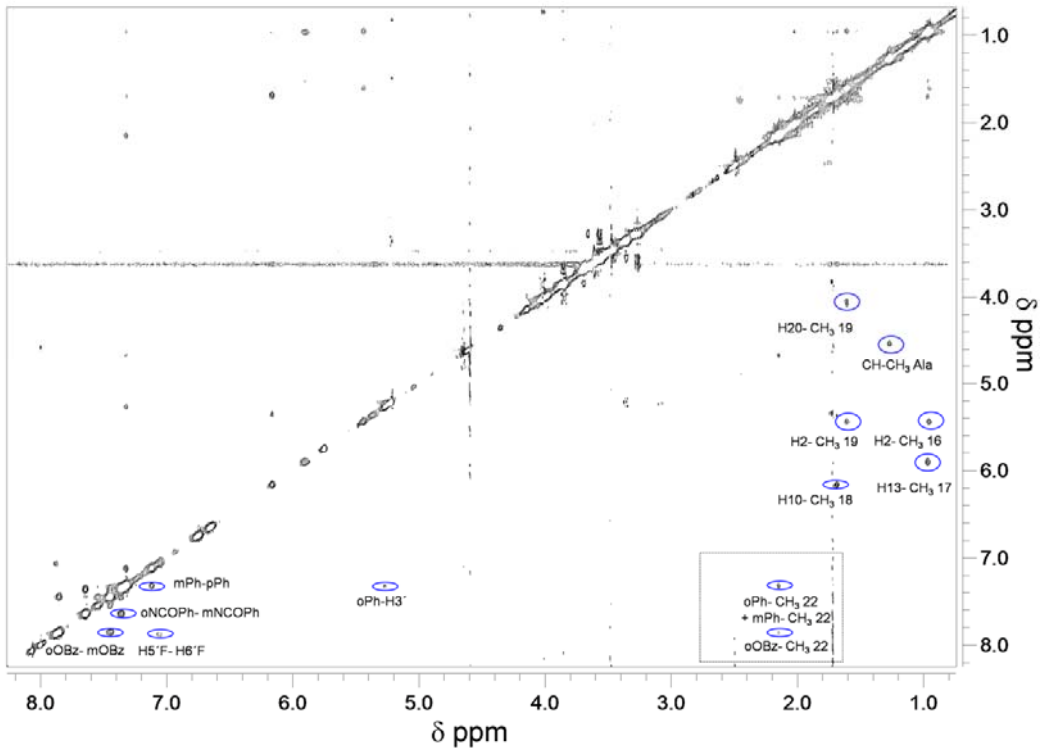
H20- CH3 19
CH-CH3 Ala
H2- CH3 19
H2- CH3 16
H13- CH3 17
H10- CH3 18
mPh-pPh
oNCOPh- mNCOPh
oOBz- mOBz
H5´F- H6´F
oPh-H3´
oPh- CH3 22
+ mPh- CH3 22
oOBz- CH3 22
δ ppm
δ ppm

Figure S1

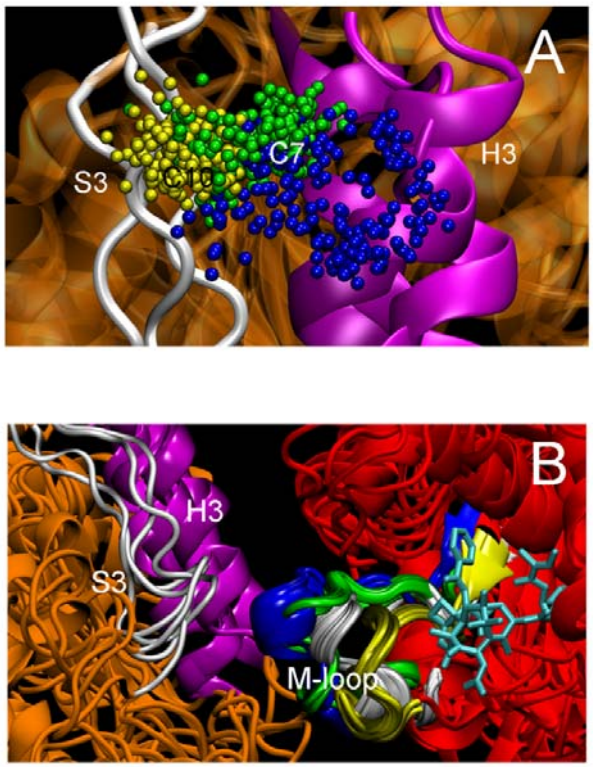

Figure S2